

# Separation of Carbon Dioxide from Synthesis Gas Containing Steam by Pressure Swing Adsorption at Mid-high Temperature

Cheng-tung Chou, Yu-Hau Shih, Yu-Jie Huang and Hong-sung Yang

**Abstract** This study aimed to utilize a pressure swing adsorption (PSA) process to capture CO<sub>2</sub> from synthesis gas, which is the effluent stream of water-gas-shift reactor. The PSA process studied is a single-bed four-step process at mid-high temperature using K<sub>2</sub>CO<sub>3</sub>-promoted hydrotalcite as adsorbent. The breakthrough curve and desorption curve were verified against the simulation program which our group developed. It uses the method of lines combined with upwind differences, cubic spline approximation and LSODE of ODEPACK software to solve the equations. The optimal operating condition is obtained by varying the operating variables, such as feed pressure, bed length, etc. Furthermore, single-bed four-step process could achieve 98.49 % recovery of H<sub>2</sub> as the top product and 96.42 % purity and 96.57 % recovery of CO<sub>2</sub> as the bottom product.

**Keywords** Pressure swing adsorption · CO<sub>2</sub> capture · Synthesis gas

## 1 Introduction

Carbon dioxide is considered to be one of the major greenhouse gases that is directly influencing the global climate changes. The United Nations Intergovernmental Panel on Climate Change (IPCC) has studied these problems and a general conclusion has been achieved between researchers, industry leaders, and politicians that dramatic reduction in greenhouse gas emissions must be achieved in order to stop climatic changes [1, 4]. So using coal more efficiently and turning it into a clean energy source is an important issue for the whole world. An integrated

---

C.-t. Chou (✉) · Y.-H. Shih · Y.-J. Huang  
Department of Chemical and Materials Engineering, National Central University,  
Jhong-Li, Taiwan  
e-mail: t310030@ncu.edu.tw

H.-s. Yang  
Center for General Education, Hwa-Hsia Institute of Technology, New Taipei City, Taiwan

gasification combined cycle (IGCC) is a potential electric power technology that turns coal into synthesis gas, which can be burned to generate power.

The CO composition in syngas reacts with steam to generate CO<sub>2</sub> and H<sub>2</sub> via the water-gas-shift reaction,  $\text{CO} + \text{H}_2\text{O} \rightarrow \text{CO}_2 + \text{H}_2$ . In this study, pressure swing adsorption (PSA) is utilized to capture CO<sub>2</sub> from the effluent stream of water-gas-shift reaction at mid-high temperature, and the purified H<sub>2</sub> can be sent to gas turbine for generating electrical power or can be used for other energy source. This technology consists of gas adsorption at high pressure and desorption at low pressure to produce high-purity products. Conventionally, PSA is used to separate CO<sub>2</sub> and H<sub>2</sub> at ambient temperature. For traditional physical adsorbent, such as zeolite and activated carbon, the adsorbed amount of CO<sub>2</sub> is too low to separate CO<sub>2</sub>/H<sub>2</sub> at mid-high temperature. Because the outlet stream from water-gas-shift reactor is already at nearly 400 °C, in order to avoid separating CO<sub>2</sub> and H<sub>2</sub> at ambient temperature, and later raise the temperature of H<sub>2</sub> for power generation, which will cause energy waste, in this study PSA processes with K<sub>2</sub>CO<sub>3</sub>-promoted hydrotalcite adsorbent are studied to capture CO<sub>2</sub> from the outlet stream of water-gas-shift reactor at 400 °C. According to literature [6], K<sub>2</sub>CO<sub>3</sub>-promoted hydrotalcite is a chemisorbent that adsorbs CO<sub>2</sub> at mid-high temperature and it does not adsorb other gases, such as CO, H<sub>2</sub> and H<sub>2</sub>O. As required by the U.S. Department of Energy, it is important to be able to concentrate the captured CO<sub>2</sub> into >90 % concentration that is suitable for underground storage.

The feed gas entering the PSA process consists of CO, CO<sub>2</sub>, H<sub>2</sub> and H<sub>2</sub>O according to National Energy Technology Laboratory report [8].

Most PSA papers assume that steam is removed before entering CO<sub>2</sub>-capture PSA process. In this study we intend to consider the steam composition in feed gas into PSA process for real-case study.

## 2 Methodology

### 2.1 Mathematical Modelling

In the non-isothermal dynamic model, the following assumptions are made:

1. The linear driving force model is used because mass transfer resistance between the gas phase and solid phase exists.
2. Only CO<sub>2</sub> is adsorbed in K<sub>2</sub>CO<sub>3</sub>-promoted hydrotalcite.
3. The ideal gas law is applicable.
4. Adiabatic system.
5. Only axial concentration and temperature gradient are considered.
6. The pressure drop along the bed can be neglected due to large particle size.

These assumptions are used in the following equations:

Overall mass balance:

$$-\frac{\partial q}{\partial z} = \frac{\varepsilon A}{R} \frac{\partial(P/T)}{\partial t} + (1 - \varepsilon)A \sum_{i=1}^n \frac{\partial n_i}{\partial t} \quad (1)$$

Mass balance for component  $i$ :

$$\frac{\partial}{\partial z} \left( \frac{\varepsilon A D_{ax,i} P}{RT} \frac{\partial y_i}{\partial z} \right) - \frac{\partial(y_i q)}{\partial z} = \frac{\varepsilon A}{R} \frac{\partial}{\partial t} \left( \frac{y_i P}{T} \right) + (1 - \varepsilon)A \frac{\partial n_i}{\partial t} \quad (2)$$

Energy balance:

$$\begin{aligned} (A\bar{k}) \frac{\partial^2 T}{\partial z^2} - \frac{\partial}{\partial z} (\bar{C}_p q T) - \pi D h (T - T_\infty) \\ = \frac{\varepsilon A}{R} \frac{\partial}{\partial t} (\bar{C}_p P) + (1 - \varepsilon)A \sum_{i=1}^n \frac{\partial}{\partial t} [n_i (\bar{C}_{pi} T - H_i)] + (1 - \varepsilon) \rho_s \bar{C}_{ps} A \frac{\partial T}{\partial t} \end{aligned} \quad (3)$$

Linear driving force model:

$$\frac{\partial N_i}{\partial t} = K_{LDF} (N_i^* - N_i) \quad (4)$$

Axial dispersion coefficient [9]:

$$D_{ax,i} = \gamma D_{m,i} + \frac{0.5 \bar{u} d_p}{1 + \beta (D_{m,i} / \bar{u} d_p)} \quad (5)$$

$$\gamma \cong 0.75, \beta \cong 9.5, \bar{u} = \frac{u_0}{e}$$

for  $0.008 < \text{Re} < 400$  and  $0.25 < \text{Sc} < 2.2$

$D_{m,i}$  can be obtained by Chapman-Enskog equation [2]:

$$\frac{D_{m,i}}{D_{m,i}^0} = \left( \frac{P_0}{P} \right) \left( \frac{T}{T_0} \right)^{\frac{3}{2}} \quad (6)$$

where  $D_{m,i}^0$  is at  $P_0$  and  $T_0$

The adiabatic system means that there is no heat transfer between bed and surrounding so that  $h = 0$  in Eq. (3).

Boundary conditions can be assumed as follows:

At the inlet end:

$$c(t, 0) = c_{in}(t), T(t, 0) = T_{in}(t) \quad (7)$$

At the outlet end:

$$\frac{\partial c(t, L)}{\partial z} = 0, \frac{\partial T(t, L)}{\partial Z} = 0 \quad (8)$$

The flow rates at the two ends of the bed are estimated by using the valve equation recommended by Fluid Controls Institute Inc.:

$$q' = 16.05 C_v \sqrt{\frac{(P_1^2 - P_2^2)}{SG \times T}} \quad \text{for } P_2 > 0.53 P_1 \quad (9)$$

$$q' = 13.61 C_v P_1 \sqrt{\frac{1}{SG \times T}} \quad \text{for } P_2 \leq 0.53 P_1 \quad (10)$$

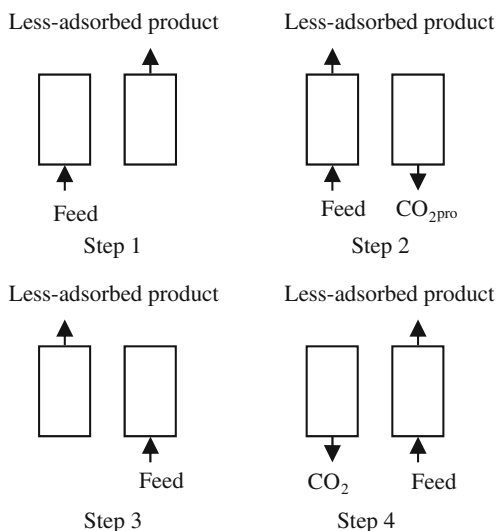
Twenty-one basic grid points are marked in the bed to set up the initial concentration, initial temperature, and initial pressure. The partial differential equations are converted to ordinary differential equations by the method of lines. The spatial derivatives of the concentration and the gas temperature are evaluated by upwind differences at every grid point. The cubic spline approximation is used to estimate the flow rates in the adsorptive bed. The concentration, temperature, and adsorption quantity in the bed are integrated with respect to time by LSODE of ODEPACK software with a time step of 0.1 s. The simulation is stopped by using Eq. 11 when the system reaches a cyclic steady state.

$$\sum \left( 1 - \frac{Y(\text{last cycle})}{Y(\text{this cycle})} \right)^2 < 1 \times 10^{-4} \quad (11)$$

where Y is the value of the mole fraction of each component and the amount of every flow stream.

## 2.2 PSA Process

The PSA process studied is a single-bed four-step process at mid-high temperature using  $K_2CO_3$ -promoted hydrotalcite. The feed gas is from the effluent stream in the water-gas-shift reactor which is cited in the report of National Energy Technology Laboratory [8]. The feed gas entering the PSA process consists of 27 %  $H_2O$ , 5 %  $CO$ , 28 %  $CO_2$  and 40 %  $H_2$ . The process is described as follows: feed pressurization (I), high pressure adsorption (II), cocurrent depressurization (III), vacuum desorption (IV). During step (I), the bed pressure increases from atmospheric pressure to high pressure, and less-adsorbed products are produced. Strongly adsorptive carbon dioxide is produced during step (IV) when the bed pressure decreases from high pressure to low pressure (0.1 atm). The procedure of the sing-bed four-step process is shown in Fig. 1. The step time and the physical parameters of adsorption bed are shown in Tables 1 and 2.

**Fig. 1** Procedure of single-bed four-step PSA process

**Table 1** Step time for single-bed four-step process

(I)	10 s
(II)	39 s
(III)	10 s
(IV)	39 s

**Table 2** Physical parameters of bed

Bed length(cm)	100
Bed diameter(cm)	100
Adsorbent density(g/cm <sup>3</sup> )	1.563 <sup>a</sup>
Adsorbent heat capacity(J/g.K)	0.85 <sup>a</sup>
Bed void	0.37
Operating temperature(K)	673.14
Feed pressure(atm)	25
Vacuum pressure(atm)	0.1

<sup>a</sup> [3]

Isotherm of K<sub>2</sub>CO<sub>3</sub>-promoted hydrotalcite was measured at 400 °C in the pressure range of 0–3 atm by Lee et al. [6] and shown in Fig. 2. The figure also shows the best fit of the CO<sub>2</sub> chemisorption isotherms using the following Eq. (12). The parameters of model for sorption of CO<sub>2</sub> are given in Table 3.

$$n_i^*(P, T) = \frac{mK_C P [1 + (a + 1)K_R P^a]}{[1 + K_C P + K_C K_R P^{(a+1)}]} \quad (12)$$

**Fig. 2** CO<sub>2</sub> chemisorption isotherm on K<sub>2</sub>CO<sub>3</sub>-promoted hydrotalcite at 400 °C [6]

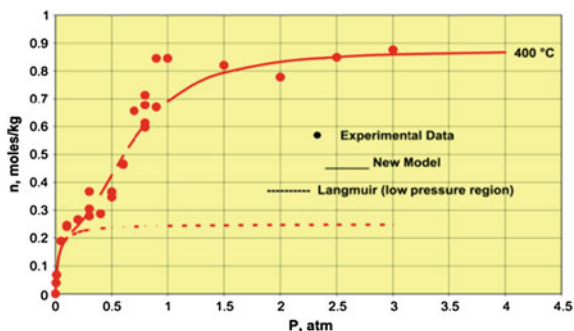


**Table 3** Parameters of model for sorption of CO<sub>2</sub> on K<sub>2</sub>CO<sub>3</sub>-promoted hydrotalcite

m(mole/kg)	0.25
a	2.5
q <sub>c</sub> (J/mole)	2.098 × 10 <sup>4</sup>
ΔH <sub>R</sub> (J/mole)	4.210 × 10 <sup>4</sup>
k <sub>c</sub> (atm <sup>-1</sup> )	37.4
k <sub>R</sub> (atm <sup>-a</sup> )	2.5

## 3 Results and Discussion

### 3.1 Simulation Verification

The breakthrough curve studied by [6] was used to verify the simulation program. A single-bed adsorption instrument was constructed to measure CO<sub>2</sub> chemisorption isotherm and CO<sub>2</sub> sorption breakthrough curves at temperature of 673.14 K on the K<sub>2</sub>CO<sub>3</sub>-promoted hydrotalcite. The single-bed was surrounded by heating elements, gas heating, cooling exchangers and flow measuring devices. A thick layer of insulation was surrounding around the column. Three thermocouples were used to measure the single-bed temperature. The exit end of column was equipped with CO<sub>2</sub> analyzers which was used to measure carbon dioxide concentration with time. The column was fully packed with the K<sub>2</sub>CO<sub>3</sub>-promoted hydrotalcite for measurement of CO<sub>2</sub> sorption dynamics. The sorbent was cleaned by flowing pure N<sub>2</sub>. At the same time the column was preheated to temperature at 673.14 K, pressure at 1 atm until no impurity flowed out in the effluent gas. Different compositions of CO<sub>2</sub> + N<sub>2</sub> mixtures were used as the feed gas. The operating conditions used are given in Table 4. The results are shown in Figs. 3, 4, 5. It shows that the simulation results are very close to experiment data. Therefore, the simulation program can be trusted.

**Table 4** Operating parameters of breakthrough curve simulation

Operating pressure (atm)	1
Operating temperature (K)	673.14
Feed flow rate (L/min)	$5.0 \times 10^{-3}$
Bed length (cm)	101.6
Bed diameter (cm)	1.73
Bed volume (L)	0.238
Bulk density (g/cm <sup>3</sup> )	0.82
Adsorption Time Constant (min <sup>-1</sup> )	3.0
Feed composition	(40 % CO <sub>2</sub> , 60 % N <sub>2</sub> ) (50 % CO <sub>2</sub> , 50 % N <sub>2</sub> ) (60 % CO <sub>2</sub> , 40 % N <sub>2</sub> )

**Fig. 3** Simulation of breakthrough curve (inlet CO<sub>2</sub> mol fraction = 0.4)

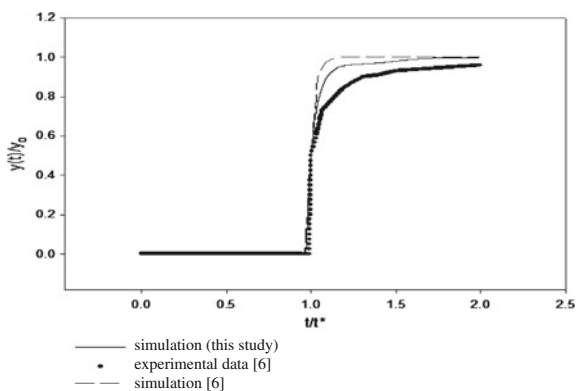


**Fig. 4** Simulation of breakthrough curve (inlet CO<sub>2</sub> mol fraction = 0.5)

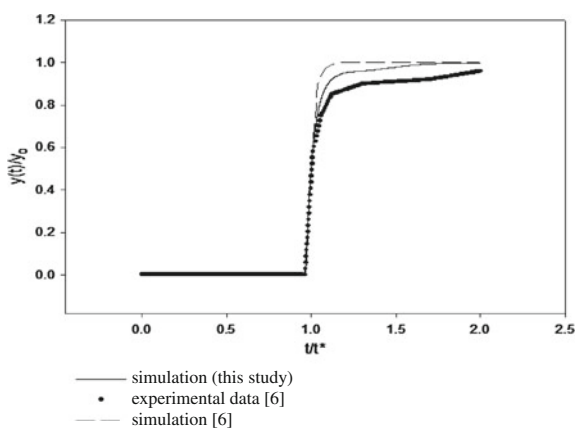
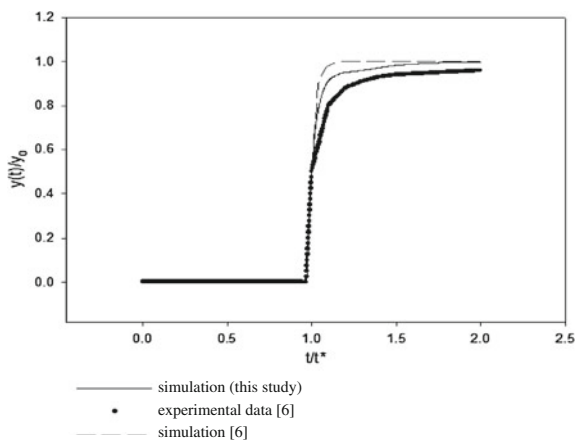


**Fig. 5** Simulation of breakthrough curve (inlet  $\text{CO}_2$  mol fraction = 0.6)



The desorption curve studied by [7] was also compared to our simulation. Figure 6 shows the column dynamic data (fraction of  $\text{CO}_2$  desorbed as a function of inlet  $\text{N}_2$  purge gas quantity) for desorption of 40 %  $\text{CO}_2 + \text{N}_2$  by  $\text{N}_2$  purge. The operating conditions used are given in Table 5. The agreement between our simulation and the experimental data is pretty good.

### 3.2 Single-Bed Four-Step PSA Process Simulation

In this study, the optimal operating conditions are discussed by varying the operating variables, such as feed pressure, bed length, vacuum pressure, feed flow rate, high pressure adsorption time and vacuum desorption time.

**Fig. 6** Simulation of desorption curve

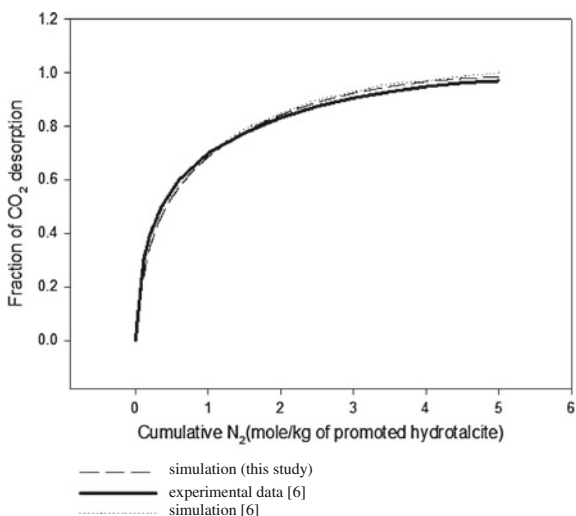


**Table 5** Operating parameters of desorption curve simulation

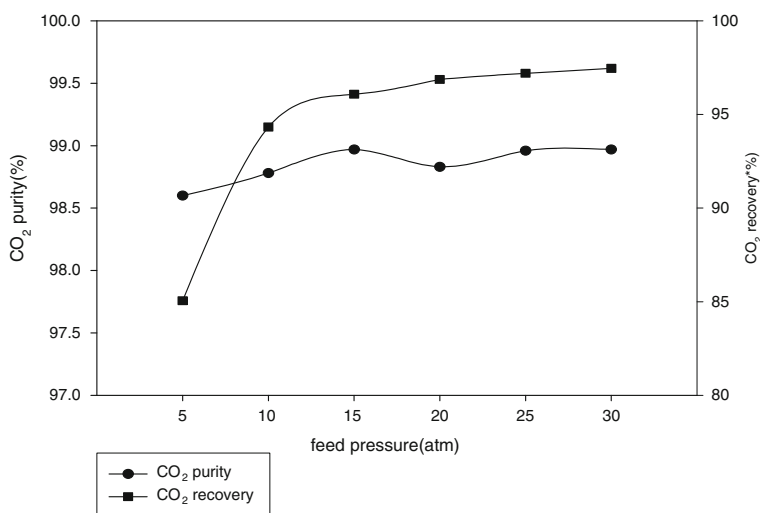
Operating pressure(atm)	1
Operating temperature(K)	793.14
Feed flow rate(L/min)	$6.667 \times 10^{-3}$
Bed length(cm)	100
Bed diameter(cm)	1.73
Bulk density(g/cm <sup>3</sup> )	0.82
Initial gas phase concentration	40 %CO <sub>2</sub> /N <sub>2</sub>

Definition of the recovery is:

$$\text{Recovery} = \frac{\text{product flow per cycle} \times \text{product concentration feed}}{\text{flow per cycle} \times \text{feed concentration}}$$

**Feed Pressure.** All the operating variables such as vacuum pressure, bed length, feed rate and step time are fixed, except feed pressure. Because the amount of gas adsorbed on K<sub>2</sub>CO<sub>3</sub>-promoted hydrotalcite increases as feed pressure increases, the flow of the strong adsorptive component to the bottom of the bed during desorption increases. Figure 7 shows that as feed pressure increases, the CO<sub>2</sub> purity and recovery in bottom product increases because CO<sub>2</sub> adsorption quantity becomes larger.

**Bed Length.** All the operating variables are fixed except bed length. With increasing bed length, the amount of adsorbent and the amount of adsorbed gas increase. Figure 8 shows that as bed length decreases, the CO<sub>2</sub> purity increases due

**Fig. 7** Effect of feed pressure on CO<sub>2</sub> in bottom product

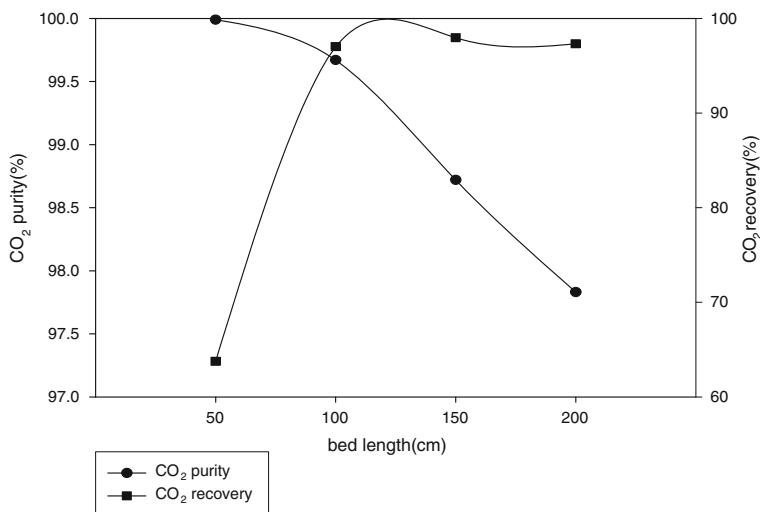


**Fig. 8** Effect of bed length on CO<sub>2</sub> in bottom product

to that the amount of CO<sub>2</sub> flow to the top product increases. At the same feed flow rate CO<sub>2</sub> recovery decreases due to that the amount of CO<sub>2</sub> flow to the top product increases.

**Vacuum Pressure.** All the operating variables are fixed except vacuum pressure. As the vacuum pressure increases, the amount of desorption gas at desorption step decreases. Figure 9 shows that as the vacuum pressure increases, the CO<sub>2</sub> recovery decreases due to that the amount of adsorbed gas flow to the bottom product at desorption step decreases.

**Feed Flow Rate.** All the operating variables are fixed except feed flow rate. As the feed flow rate increases, the amount of CO<sub>2</sub> increases at high pressure adsorption step. Figure 10 shows that as the feed flow rate increases, the CO<sub>2</sub> recovery decreases due to that the amount of adsorption/desorption are approximately fixed. The CO<sub>2</sub> purity increases as the amount of adsorbed gas increases.

**High Pressure Adsorption Time and Vacuum Desorption Time.** All the operating variables are fixed except high pressure adsorption time/vacuum desorption time. The amount of CO<sub>2</sub> increases in the column as the pressure adsorption time increases. Therefore, Fig. 11 shows that CO<sub>2</sub> recovery decreases with the decreasing 2nd/4th step time.

The best operating conditions for the single-bed four-step PSA process at mid-high temperature is shown in Fig. 12. The results of best operating condition for the single-bed four-step process at mid-high temperature are 96.42 % purity and 96.57 % recovery of CO<sub>2</sub> as bottom product as shown in Fig. 12.

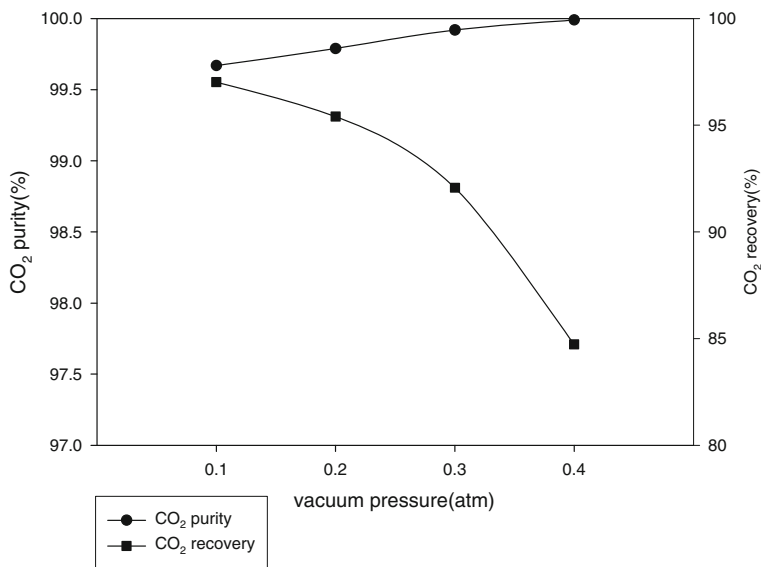


Fig. 9 Effect of bed length on CO<sub>2</sub> in bottom product

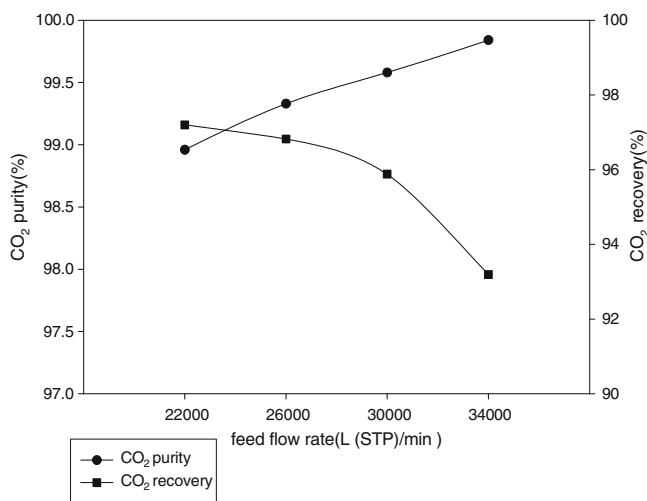


Fig. 10 Effect of feed flow rate on CO<sub>2</sub> in bottom product

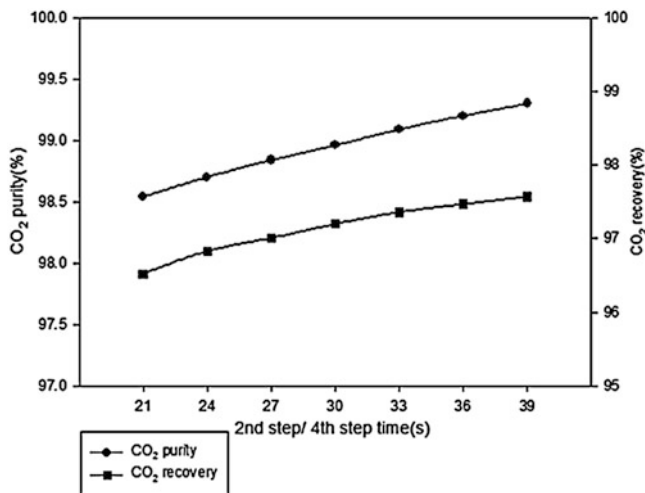
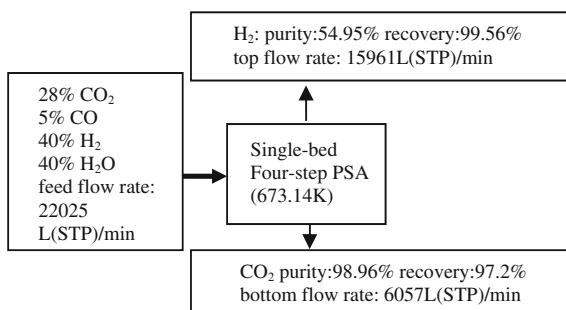


Fig. 11 Effect of 2nd/4th step time on CO<sub>2</sub> in bottom product

Fig. 12 Results of the single-bed four-step PSA process at mid-high temperature



### 4 Conclusions

A single-bed four-step pressure swing adsorption process is explored in this simulation study. The adsorbent K<sub>2</sub>CO<sub>3</sub>-promoted hydrotalcite was used [6]. The accuracy of the simulation program is verified by comparing our simulation results with the experimental data of breakthrough curve and desorption curve from Lee et al. [6, 7] and the single-bed five-step PSA results of Kim et al. [5]. The optimal operating condition is obtained by varying the operating variables, such as feed pressure, bed length, feed flow rate, etc. Furthermore, the optimal operating condition for inlet (27 % H<sub>2</sub>O, 5 % CO, 28 % CO<sub>2</sub> and 40 % H<sub>2</sub>) at mid-high temperature 673 K and bed diameter 100 cm is bed length 200 cm, feed pressure 25 atm, vacuum pressure 0.1 atm and step times at 10, 30, 10 and 30 s. The best results and the optimal operating condition for the single-bed four-step PSA process

**Table 6** Optimal operating condition for the single-bed four-step PSA process at mid-high temperature

Feed pressure (atm)	25
Bed length (cm)	100
Vacuum pressure (atm)	0.1
Feed flow rate (LSTP/min)	22000
High pressure adsorption time and vacuum desorption time (s)	30

at mid-high temperature are shown in Fig. 12 and Table 6. In the future, our research will proceed with dealing the top stream from CO<sub>2</sub>-PSA by a second stage H<sub>2</sub>-PSA to improve H<sub>2</sub> purity.

**Acknowledgments** The authors wish to thank the financial support from National Science Council, Taiwan under project number NSC 102-3113-P-008 -007.

## References

1. Abu-Zahra MRM, Feron PHM, Jansens PJ, Goetheer ELV (2009) New process concepts for CO<sub>2</sub> post-combustion capture process integrated with co-production of hydrogen. *Int J Hydrogen Energy* 34:3992–4004
2. Bird RB, Stewart WE, Lightfoot EN (1960) *Transport phenomena*. Wiley, New York
3. Ding Y, Alpay E (2000) Equilibria and kinetics of CO<sub>2</sub> adsorption on hydrotalcite adsorbent. *Chem Eng Sci* 55:3461–3474
4. IPCC (Intergovernmental Panel on Climate Change) (2005) *Carbon dioxide capture and storage*. Cambridge University Press, Cambridge
5. Kim WG, Yang J, Han S, Cho C, Lee CH, Lee H (1995) Experimental and theoretical study on H<sub>2</sub>/CO<sub>2</sub> separation by a five-step one-column PSA processes. *Korean J Chem Eng* 12:503–511
6. Lee KB, Caram HS, Verdooren A, Sircar S (2007) Chemisorption of carbon dioxide on potassium carbonate promoted hydrotalcite. *J Colloid Int Sci* 308:30–39
7. Lee KB, Beaver MG, Caram HS, Sircar S (2007) Reversible chemisorption of carbon dioxide: simultaneous production of fuel-cell grade H<sub>2</sub> and compressed CO<sub>2</sub> from synthesis gas. *Adsorption* 13:385–392
8. NETL (National Energy Technology Laboratory) (2009) Evaluation of alternate water gas shift configurations for IGCC systems, DOE/NETL-401/080509
9. Wen CY, Fan LT (1976) Models for flow systems and chemical reactors. *J AIChE* 22:412